



## Relationships between foliation development, porphyroblast growth and large-scale folding in a metaturbidite suite, Snow Lake, Canada

JÜRGEN KRAUS and PAUL F. WILLIAMS

Department of Geology, The University of New Brunswick, P.O. Box 4400, Fredericton, NB, Canada E3B 5A3

(Received 28 February 1997; accepted in revised form 13 October 1997)

**Abstract**—Complex relationships exist between cleavage development, metamorphism and large-scale folding in the well-bedded, polydeformed, staurolite-grade metaturbidite of the Burntwood Suite, internal Paleoproterozoic Trans-Hudson Orogen at Snow Lake, Manitoba, Canada. It is demonstrated: (a) that cleavage in anisotropic pelitic rock develops whenever microfolding is possible and that, commonly, initiation of a cleavage, which is pervasive on the scale of a fold, predates folding; (b) how a new axial planar fabric can develop on one fold limb of a symmetrical fold and not on the other; and (c) how two cleavages of different generations can be present in adjacent beds. It is further shown that porphyroblasts rotate with respect to geographical coordinates during folding. Finally, dissolution of cleavage septa is suggested here as an alternative mechanism for the generation of schistosity. The Burntwood Suite is exposed on the dismembered limb of a macroscopic, isoclinal  $F_2$  structure and preserves a domainal cleavage ( $S_2$ ), which locally grades into a schistosity.  $S_2$  developed from crenulation of a generally bedding-parallel  $S_1$  cleavage that is axial planar to  $F_1$  isoclinal folds formed at 1.84 Ga. Porphyroblast growth coincided with crenulation of  $S_1$  early during  $F_2$  folding at 1.815–1.8 Ga. Early stages of  $S_2$  development are recorded by inclusion trails ( $S_i$ ) in the porphyroblasts. During  $F_2$  flexural-flow folding, variations in magnitude of bedding-parallel shear in lithologies of different competency resulted in a strong  $S_2$  refraction and thus heterogeneous strains between beds. Independent of shear magnitude and resulting  $S_0/S_2$  angle,  $S_i$  and  $S_2$  remained sub-orthogonal everywhere, and thus porphyroblasts and the enveloping  $S_2$  rotated by equal amounts with respect to  $S_0$ . As the different magnitudes of porphyroblast rotation in different beds could not be exactly balanced by the counteracting rotation of the fold limbs (same magnitude for all beds) during fold tightening, most porphyroblasts also rotated with respect to geographical coordinates.  $S_2$  was crenulated prior to  $F_3$  large-scale folding, where favourably oriented.  $F_3$  crenulations were tightened on the eastern  $F_3$  limb and unfolded by sinistral layer-parallel shear on the western limb, where  $F_2$  and  $F_3$  layer-parallel shears were of opposite and the same sense, respectively. As a result, the initial developmental stages of an  $S_3$  are developed only on the eastern  $F_3$  limb, and there only in incompetent layers, whereas  $S_2$  is preserved in the competent layers. On the western limb,  $S_2$  is preserved and appears axial planar to the  $F_3$  structure. The  $S_2$  domainal fabric was locally transformed into a schistosity by dissolution of the septa during widespread fluid activity, which endured until syn- or post- $F_3$ . © 1998 Elsevier Science Ltd.

### INTRODUCTION

Cleavage formation in strongly anisotropic micaceous pelitic rocks is regarded essentially as a crenulation process (e.g. Williams, 1972, 1977, 1979, 1990; Weber, 1976, 1981; Knipe and White, 1977). Microfolding of a sedimentary or tectonic foliation leads to a crenulation fabric. Crenulation is believed to initiate prior to or during the initial stages of large-scale folding. Thus, if the earlier fabric was approximately bedding-parallel, the crenulations form with their axial planes at a high angle to bedding (e.g. Kienow, 1942; Williams, 1972, 1979; Knipe and White, 1977; Nickelsen, 1979; Weber, 1981; Williams and Schoneveld, 1981; Henderson *et al.*, 1986; Wright and Henderson, 1992).

During cleavage development, one or more of three competing metamorphic processes are generally operative to varying degrees: (1) solution transfer, (2) recrystallization and (3) neocrystallization (e.g. Rickard, 1961; Williams, 1972, 1977, 1990; Marlow and Etheridge, 1977; Knipe, 1981). As a result, the final fabric might be a domainal fabric such as differentiated crenulation cleavage, differentiated layering (e.g. Williams, 1972, 1990), domainal slaty cleavage (e.g. Hoeppe-

ner, 1956; Hobbs *et al.*, 1976, p. 222), or a penetrative fabric such as a penetrative slaty cleavage (e.g. Williams, 1972, 1977; Hobbs *et al.*, 1976, p. 222) or a schistosity (e.g. Williams, 1977, 1985). Undifferentiated crenulation cleavages (not to be confused with crenulation that has not developed into a true cleavage) appear to be the exception.

Cleavage-forming mechanisms and the relationship between fabric development and folding are commonly studied in low-grade rocks, where the phyllosilicates do not experience coarsening. Low-grade rocks, unfortunately, generally lack porphyroblasts, which are useful for establishing the relative timing of deformation and metamorphism. Particularly useful are synkinematic porphyroblasts, which preserve stages of fabric development as inclusion trails ( $S_i$ ). The relationship between  $S_i$  and the foliation external to the porphyroblast ( $S_e$ ) is in some cases ambiguous, especially where  $S_i$  and  $S_e$  are discontinuous. This relationship has therefore been the subject of extensive discussion (e.g. Zwart, 1960, 1962; Spry, 1969; Vernon, 1977, 1978, 1988, 1989; Bell, 1985; Williams, 1985; Bell *et al.*, 1986, 1992c; Passchier *et al.*, 1992; Johnson and Vernon, 1995). Since the early 1980s, many of the microfabric studies in medium-grade pelitic

rocks have focussed on (1) porphyroblast–matrix relationships *per se* in order to correlate metamorphic events with stages of foliation formation, and (2) the question of whether porphyroblasts rotate or not with respect to the enveloping fabric and/or geographical coordinates (e.g. Bell, 1985; Vernon, 1988; Bell *et al.*, 1992a–c; Passchier *et al.*, 1992; Johnson and Vernon, 1995). In most of these studies the porphyroblast–cleavage relationships were not considered in the context of associated mesoscopic and macroscopic structures. However, we regard such relationships as important tools for the delineation of the tectonometamorphic history of an area. Evaluating porphyroblast–matrix relationships around a fold can also help eliminate at least some  $S_i/S_c$  ambiguities, as demonstrated by Williams (1985).

In the present paper we establish complex relationships between the development and overprinting of the regional  $S_2$  cleavage, porphyroblast growth and two phases of large-scale folding ( $F_2$  and  $F_3$ ) in a well-bedded metaturbidite sequence at Snow Lake, Canada. In order to extract the maximum information from the rock, the porphyroblast–matrix relationships were studied across a portion of heterogeneously deformed layering, which shows strong cleavage refraction. Selective overprinting of the cleavage, where favourably oriented, by subsequent  $F_3$  crenulation, is helpful in eliminating ambiguous porphyroblast–matrix relationships and gives evidence of cleavage initiation during layer-parallel shortening prior to, or in the early stages of,  $F_2$  folding. It is further shown how an axial planar cleavage may develop on one fold limb only and how different generations of cleavage may be present in adjacent beds. Moreover, it can be demonstrated that dissolution of  $S_2$  cleavage septa defined by muscovite during widespread fluid activity on the retrograde metamorphic path is responsible for the local transition of a domainal cleavage into a schistosity.

## GEOLOGICAL SETTING

The Snow Lake area is situated in a transitional zone in the Paleoproterozoic Trans-Hudson Orogen (Lewry and Stauffer, 1990) of Manitoba, Canada (Fig. 1), in which the *Snow Lake assemblage* (part of the previous Flin Flon–Snow Lake greenstone belt) and the Kiseynew domain, a former marginal basin, were interleaved during the Hudsonian Orogeny (Fig. 2) (Kraus and Williams, 1994a; Connors, 1996). This zone of interleaving is referred to as the Snow Lake allochthon (Kraus and Menard, 1997). The Snow Lake assemblage comprises rocks of island arc affinity that formed at  $\sim 1.9$  Ga (Stern *et al.*, 1995; Lucas *et al.*, 1996; David *et al.*, 1996). The Kiseynew domain consists of metamorphosed metaturbidites (*Burntwood Suite*), which are intercalated with their terrestrial facies correlative (*Missi Suite*) (Bailes, 1980; Stauffer, 1990; Zwanzig, 1990). U–Pb geochronology of detrital zircons has yielded a sedimentation age

younger than  $\sim 1.859$  Ga for the Burntwood Suite (David *et al.*, 1996) and  $\sim 1.845$  Ga for the Missi Suite (Ansdell, 1993). SW-movement of Kiseynew sedimentary basin over the Snow Lake arc (e.g. Kraus and Williams, 1994a; Connors, 1996) resulted in two phases of isoclinal folding,  $F_1$  and  $F_2$ , and related thrusting, which led to multiple repetition of the contact between the two domains (Kraus and Williams, 1994b; Connors, 1996).  $F_1$  folds are truncated by 1.84–1.83 Ga granitoid plutons (Kraus and Williams, 1995; Connors, 1996; David *et al.*, 1996).

Peak thermal conditions were reached at 1.815–1.8 Ga (Gordon *et al.*, 1990; Parent *et al.*, 1995; David *et al.*, 1996) coeval with  $F_2$  in the study area (Kraus and Menard, 1997; Menard and Gordon, 1997). Post 1.8 Ga sinistral–oblique collision of the Superior Province with the Trans-Hudson Orogen along the Thompson Nickel Belt (Hoffman, 1988; Bleeker, 1990) generated NNE-trending open  $F_3$  folds of the tectonostratigraphy (Kraus and Williams, 1994b). The large, symmetrical  $F_3$  Threehouse synform largely controls the map-scale pattern in the Snow Lake area (Fig. 2).

The rocks discussed here form a slice of Burntwood Suite metaturbidites (previously referred to as File Lake Formation by Bailes, 1980) that are exposed around the town of Snow Lake (Fig. 2). The northerly to easterly dipping slice (Fig. 3a) varies in thickness from several hundred metres to 4–5 km and is in structural contact above and below with rocks of the arc assemblage. The bounding faults are the Snow Lake fault below and the McLeod Road thrust above (Fig. 2), which are of  $F_1$  and  $F_2$  age, respectively (Kraus and Williams, 1994a; Connors, 1996). Detailed structural mapping has revealed that the slice is the dismembered lower limb of a macroscopic  $F_2$  fold (McLeod Lake fold), which was truncated along the McLeod Road thrust in the tightening stages of  $F_2$  folding (Fig. 2; see also Fig. 6c) (Kraus and Williams, 1994a). The  $F_2$  structure overprints macroscopic  $F_1$  folds and, together with the thrusts, is openly refolded by the symmetrical  $F_3$  Threehouse synform (Fig. 2). In the core of the  $F_3$  Threehouse synform at Snow Lake, all linear features are broadly coaxial plunging moderately to steeply to the NE (Fig. 3) (Kraus and Williams, 1994b). On the eastern and western limbs, bedding dips moderately to steeply in northerly and easterly directions, respectively (Fig. 3).

### Metamorphism

In the Snow Lake area, the metamorphic grade increases to the N, towards the upper tectonostratigraphic levels, from chlorite-grade at Wekusko Lake to partial melting at the southern margin of the Kiseynew domain (Figs 1 & 2) (e.g. Froese and Gasparrini, 1975; Bailes and McRitchie, 1978; Kraus and Menard, 1997; Menard and Gordon, 1997). Around the  $F_3$  Threehouse synform at Snow Lake, the turbidites are metamorphosed at staurolite-grade, containing the assemblage

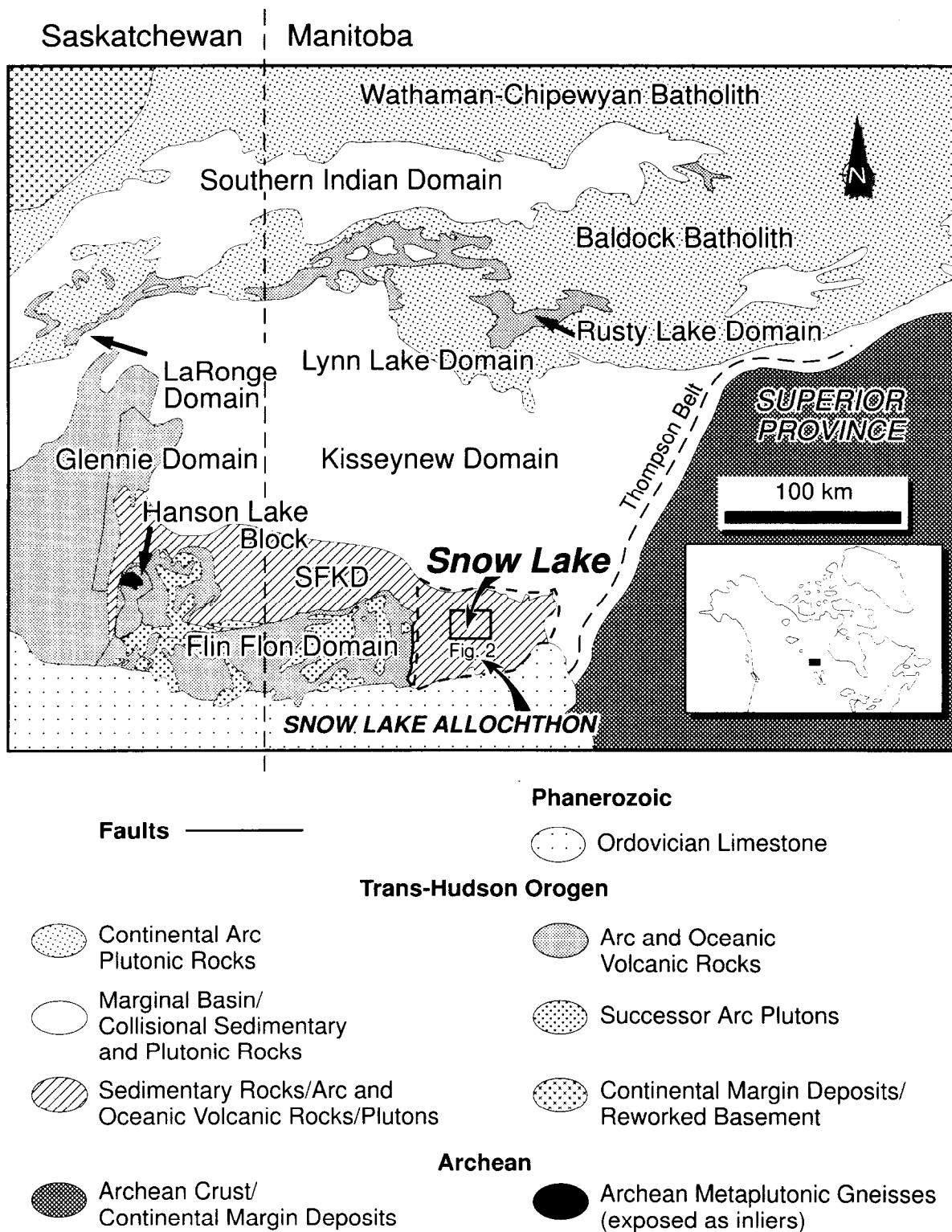


Fig. 1. Lithotectonic domains of the internal Trans-Hudson Orogen (after Hoffman, 1988). SFKD=southern flank of Kisseynew domain.

staurolite + biotite + garnet + muscovite + plagioclase + graphite ± chlorite, with minor ilmenite, rutile, pyrrhotite, tourmaline, magnetite, zircon and monazite. Chlorite is abundant only as inclusions in porphyroblasts and as a retrograde phase partially replacing biotite, and

rims of garnet and staurolite. Temperatures of 560–570°C at an associated pressure of 4–4.5 kbar were calculated on representative samples (Kraus and Menard, 1997) using the following methods: the TWQ 1.02 program (Berman, 1991) with thermodynamic data

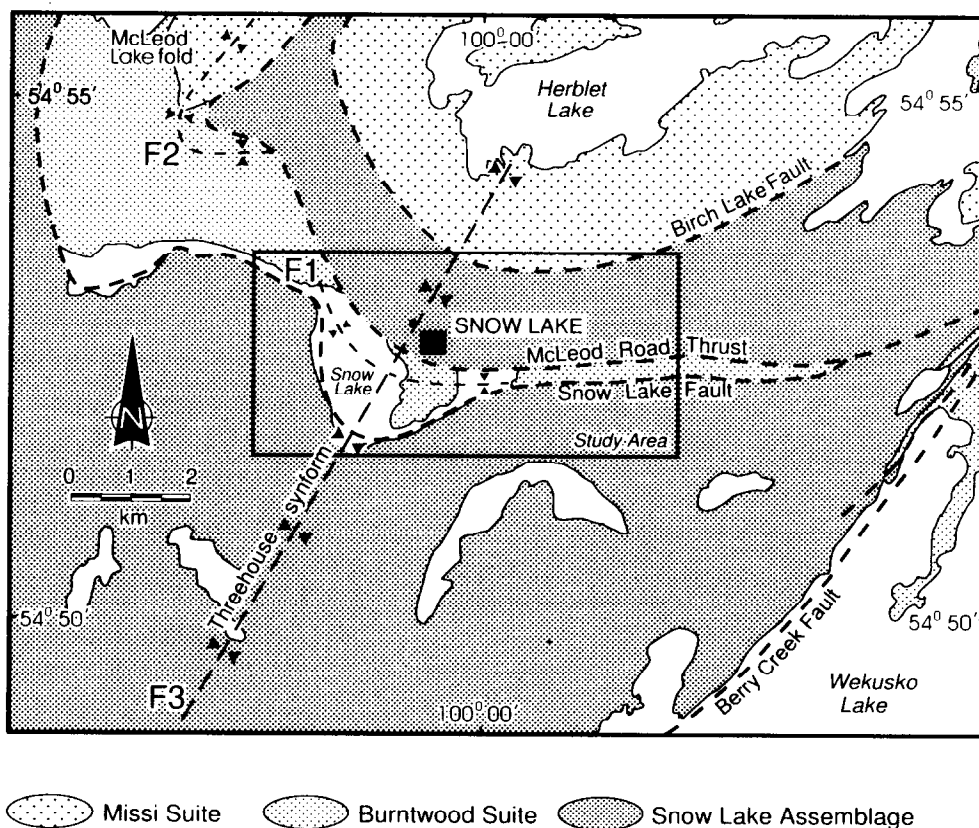


Fig. 2. Simplified geological map of the Threehouse synform area at Snow Lake.

from Berman (1988, 1990), Fuhrman and Lindsley (1988), Berman and Koziol (1991), McMullin *et al.* (1991), and Mäder *et al.* (1994); the garnet–biotite thermometer (Kleemann and Reinhardt, 1994); and the garnet–biotite–muscovite–plagioclase barometer (Hodges and Crowley, 1985; Powell and Holland, 1988; Hoisch, 1990). These results were interpreted as representing peak metamorphic conditions (Kraus and Menard, 1997).

#### *The Burntwood suite metaturbidites*

The metaturbidite sequence is composed of greywacke beds, up to 1 m thick, alternating with mudstones and siltstones. The greywacke beds have preserved grading and other primary features such as scours, rip-up clasts, calcareous concretions and rare flame structures. Locally, the Burntwood Suite appears as a pelitic schist up to several metres thick. The compositional change within graded greywacke beds is reflected in reversed grading (due to coarser grain size of metamorphic minerals in the more pelitic parts). At the base of the beds biotite (up to 2 mm) is the dominant porphyroblast phase. With increasing Al-content towards the top, euhedral to subhedral pinhead garnet (1–3 mm in diameter), and large staurolite (up to 14 cm long) become abundant.

#### CLEAVAGE DESCRIPTION

In the sequence, there is only one discrete cleavage,  $S_2$ , which appears as a small-scale differentiated layering (domainal cleavage) or a penetrative schistosity that is strongly refracted across lithological layering (Fig. 4a). In hand specimen,  $S_2$  is defined by trails of dimensionally and crystallographically well-aligned, lensoid to angular biotite of variable aspect ratio (Fig. 4a). The biotite grains are locally enveloped by thin films of muscovite.  $S_2$  streamlines around garnet and staurolite. Locally, staurolite is also aligned parallel to the cleavage, but it is commonly a magnitude larger than the cleavage domains. Many biotite and staurolite porphyroblasts are pulled apart and extended in  $S_2$ , the stretching direction being at a high angle to the  $S_0/S_2$  intersection (Fig. 4a; see also Fig. 8a). There is no cleavage in mica-poor portions of the greywackes. In thin section (*all thin sections described in this paper are cut perpendicular to the  $S_0/S_2$  intersection*),  $S_2$  shows a variety of microstructures. The domainal character of the cleavage indicates its origin as a crenulation cleavage (Fig. 4) (cf. Williams, 1972, 1990). Garnet and biotite are confined to quartz-rich domains, which constitute the microlithons (Fig. 4; see also Fig. 7). An earlier fabric ( $S_1$ ) is preserved as  $S_1$  in the porphyroblasts, the significance of which will be discussed below.  $S_2$  is

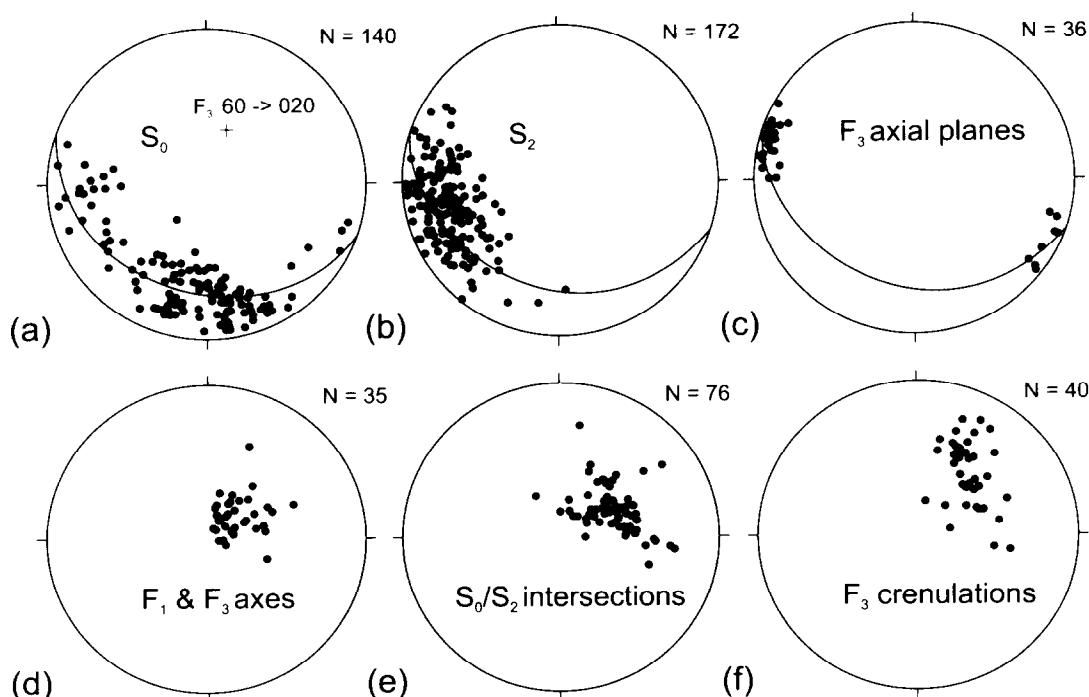


Fig. 3. Equal-area projections (lower hemisphere, Schmidt net) of structural data. (a)–(c) Foliations: (a) Poles to bedding; (b) Poles to  $S_2$ ; (c) Poles to axial planes of  $F_3$  crenulations; (d)–(f) Linear features: (d) Fold axes; (e)  $S_0/S_2$  intersection lineations (calculated); (f)  $F_3$  crenulation axes on  $S_2$ .

defined by a quartz shape fabric in the quartz-rich domains, where, in rare cases, the matrix quartz is not annealed. Thin muscovite films, which constitute the  $S_2$  septa, anastomose around the porphyroblasts (Fig. 4b–d). The basal planes of the muscovite grains are parallel to  $S_2$  in both the films and quartz-rich domains (Fig. 4b–d). Locally, closely spaced porphyroblastic biotite fish are separated by thin anastomosing muscovite films and the overall cleavage morphology resembles that of a domainal schistosity (Figs 4b & 5) (cf. Hobbs *et al.*, 1976, p. 227). The films are commonly accentuated by graphite trails, which probably resulted from passive concentration by the dissolution of quartz from the developing septa (Fig. 4c & d). At the scale of a thin section, these muscovite films are preserved in some domains of a micro-bed but may have been dissolved to varying degrees in others so that the domainal character of the fabric locally gives way to a more homogeneous distribution of aligned muscovite in the matrix (Fig. 4d). In domains strongly affected by muscovite dissolution, the overall appearance of the fabric approaches one of a penetrative schistosity (Fig. 5). Here, the former septa are locally tracked by trails of the less soluble graphite. The removal of muscovite is discussed in more detail below. Toward the base of the greywacke beds, which were initially poor in muscovite, the rare muscovite is randomly oriented or less orderly crenulated.

## CLEAVAGE–FOLD RELATIONSHIPS

### *Distribution and overprinting of cleavage in the Threehouse synform*

The deformation sequence in the study area was previously considered to comprise two phases of folding (Russell, 1957; Froese and Moore, 1980; Galley *et al.*, 1988). A first generation of isoclinal folds ( $F_1$ ) was believed to be refolded by the open Threehouse synform ( $F_2$ ; *ibid.*). The prominent regional  $S_2$  was considered to be axial planar to the Threehouse synform (*ibid.*). Our detailed structural mapping showed that the regional  $S_2$  cuts mesoscopic and macroscopic  $F_1$  folds, is axial planar to a second generation of macroscopic isoclinal folds ( $F_2$ ) (Kraus and Williams, 1994a), and is deformed by the  $F_3$  Threehouse synform (Fig. 2). Mesoscopic  $F_2$  folds are very rare. Further evidence for this deformation sequence is given by the constant sinistral asymmetry of  $S_2$  and  $S_0$  on the exposed limb of the  $F_2$  McLeod Lake fold around the  $F_3$  Threehouse synform. (*Note: all asymmetries and shear senses given in this paper refer to the  $F_2$  profile plane looking down the NE-plunging  $S_0/S_2$  intersection; the asymmetry is sinistral, if the clockwise intersection angle between  $S_0$  and  $S_2$  is  $< 90^\circ$ ; it is dextral, when the dihedral angle is  $> 90^\circ$ .*)

On both  $F_3$  limbs,  $S_0/S_2$  dihedral angles vary significantly in adjacent beds from close to  $90^\circ$  in competent

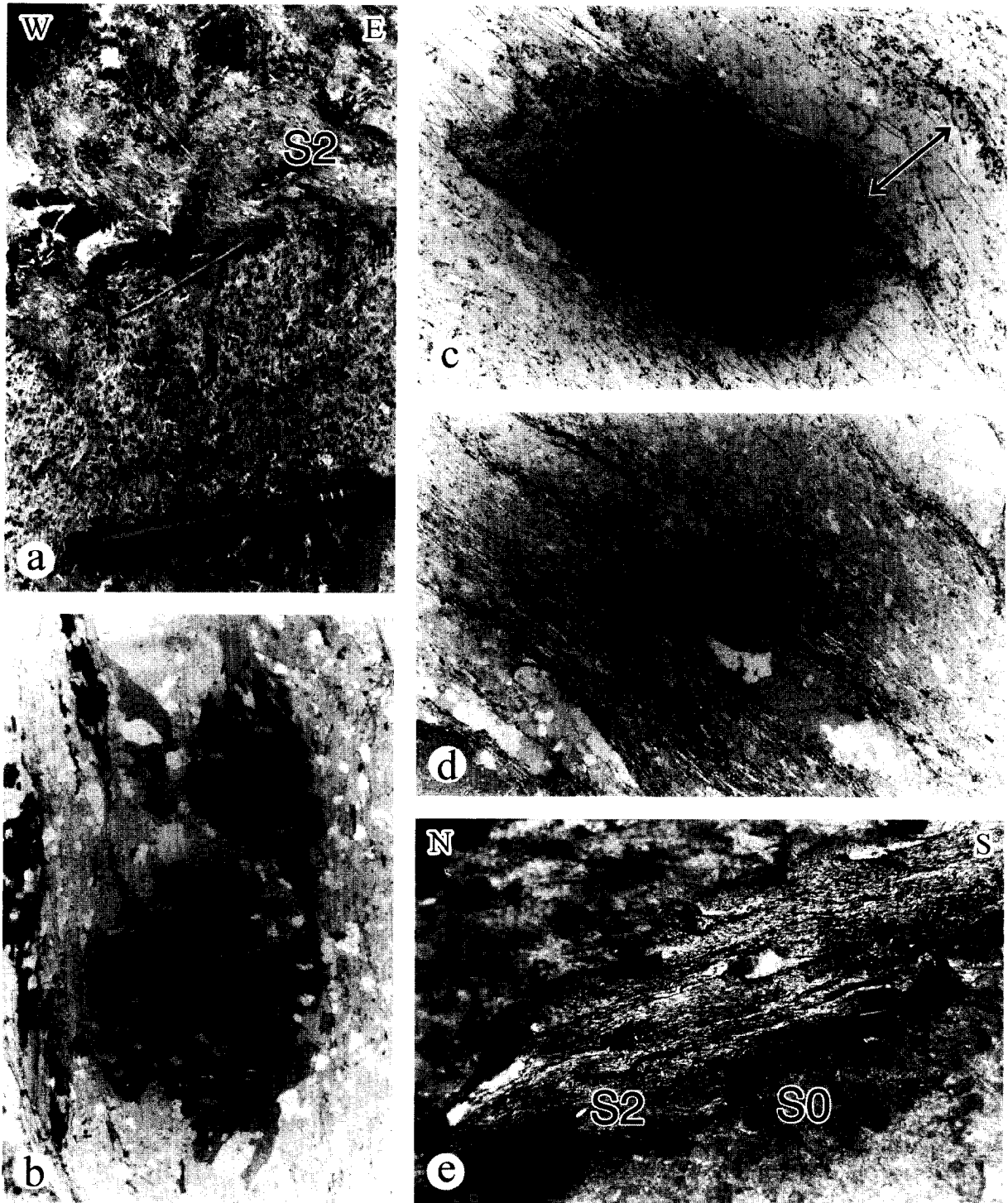


Fig. 4. (a)–(d) Bedding–cleavage–porphyroblast relationships on the Threehouse east limb (Fig. 2). (a) Refraction of domainal fabric ( $S_2$ ) across layer interface ( $S_0$ ). Upper bed:  $S_2$  and pressure-shadows of biotites (fine white strings) are refolded into Z-asymmetric open  $F_3$  crenulations. Lower bed: The high-angle  $S_2$  is undeformed. Geometrical relationships are as in Fig. 6d. (b)–(d) Photomicrographs of (a).  $S_0$  is parallel to bases of photomicrographs. (b) Lower bed:  $S_2$  domainal schistosity at high angle to  $S_0$ . Biotite fish contain planar  $S_1$  ( $= S_1$ ) of elongate quartz grains. Base is 1.7 mm. (c) Upper bed: The biotite blast overgrew S-asymmetric  $F_2$  crenulations of  $S_1$ . Note the graphitic residue (double arrow) and the depleted muscovite films. Opaque phase is ilmenite. Base is 1.1 mm. (d) Upper bed, same thin section as (c): Varying degrees of matrix homogenisation. Graphite-enriched  $S_2$  septa are preserved locally. Quartz pressure-shadows of biotite are recrystallised. Base is 4.2 mm. (e) Relict S-asymmetric  $F_3$  crenulations, Threehouse west limb.

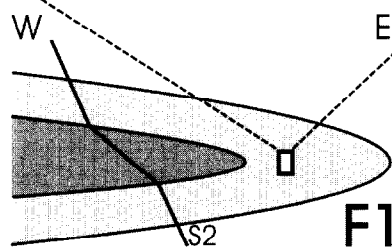


Fig. 5. Photomicrograph of porphyroblast-matrix relationships in hinge of minor  $F_1$  fold on the Threehouse east limb. Refracted  $S_2$  cuts the  $F_1$  axial surface at intermediate to high angles. Straight  $S_1$  ( $= S_1$ ) in garnet and biotite are suborthogonal to  $S_2$ . Quartz as inclusions in garnet are elongate and smaller than in the matrix. Left hand side of photomicrograph:  $S_2$  is developed as a domainal schistosity. Right hand side:  $S_2$  septa are not preserved. Base is 6.4 mm.

greywackes to  $10^\circ$  in some incompetent mudstones. On the east limb, wherever  $S_0/S_2$  angles are small,  $S_2$  is refolded by Z-asymmetrical tight to open  $F_3$  crenulations or, in micaceous portions, by kinks, whose wavelengths exceed the spacing of  $S_2$  domains considerably (Fig. 4a; see also Fig. 8a). These crenulations, which do not constitute a true cleavage, were not noted by previous writers. The axial surfaces of the crenulations are approximately axial planar to the Threehouse synform, dipping steeply ESE and containing the  $F_3$  fold axis.  $S_2$  is undeformed, where it is at a high angle to  $S_0$ .

On the west limb,  $S_0/S_2$  dihedral angles are generally smaller than in comparable lithologies on the east limb. Here,  $S_2$  is not overprinted except at three localities, where tight-gentle, S-asymmetrical  $F_3$  crenulations are developed (Fig. 4e).

### Interpretation

The reconstruction of the cleavage and folding history during  $F_2$  and  $F_3$  based on these geometrical relationships is shown in Fig. 6. It is assumed that  $S_2$  formed originally at a high angle to  $S_0$  during  $F_2$  layer-parallel shortening (Fig. 6a). This assumption is discussed below.  $S_2$  refraction occurred due to differential sinistral layer-parallel shear on the exposed lower limb of the  $F_2$  McLeod Lake fold during  $F_2$  fold development (Fig. 6b). The mudstones and incompetent portions of the graded beds maximised  $F_2$  layer-parallel shear or shear induced vorticity (Lister and Williams, 1983); the competent portions maximised  $F_2$  spin (Lister and Williams, 1983). The large-scale  $F_2$  fold was subsequently dismembered along the McLeod Road thrust (Fig. 6c). The constant sinistral  $S_0/S_2$  asymmetry across the Threehouse synform indicates that the turbidite sliver represents the southern limb of the easterly closing  $F_2$  McLeod Lake fold (Fig. 6c). During  $F_3$  folding, layer-parallel shear was of opposite sense on the opposite limbs of the Threehouse synform (Fig. 6d). Continued sinistral layer-parallel shearing on the west limb resulted in further decrease in  $S_0/S_2$  dihedral angles. Here,  $S_2$  appears to be axial planar to the Threehouse synform, because the exposed limb of the  $F_2$  structure has the same asymmetry as the western limb of the  $F_3$  synform and thus the  $F_2$  asymmetry of  $S_0$  and  $S_2$  is preserved. It is important to note that  $F_2$  and  $F_3$  must be approximately coaxial or  $S_2$  would not appear to be axial planar to  $F_3$ . This coaxiality is indicated by the poles to  $S_0$ ,  $S_2$  and the axial planes of  $F_3$  crenulations plotting on approximately the same great circle (Fig. 3a-c).

On the Threehouse east limb, the shear sense reversed from  $F_2$ -related sinistral shear to  $F_3$ -related dextral shear following initial layer-parallel shortening (Fig. 6d).  $S_2$  was in the shortening sector of the instantaneous  $F_3$ -related shear strain and, where it was at a shallow angle to  $S_0$ , the finite strain was sufficient to result in well developed open-tight crenulations. As shearing continued the crenulations were constrained to become Z-

asymmetrical. Where  $S_2$  was at a high angle it started in the shortening field but after accumulating only a small amount of shear strain it was rotated into the extensional sector. Any crenulation developed in response to the initial shortening would be unfolded. Thus the net effect is that where  $S_2$  was inclined to  $S_0$  at an angle approaching  $90^\circ$  it was not folded by  $F_3$  shear.

### Timing of crenulation initiation with respect to folding

So far, we have assumed, that crenulations form early in the folding history with axial planes at a high angle to the earlier fabric, if this earlier fabric was parallel to or at a low angle to bedding (cf. Kienow, 1942; Williams, 1972, 1979; Knipe and White, 1977; Nickelsen, 1979; Weber, 1981; Henderson *et al.*, 1986; Wright and Henderson, 1992). This assumption fits the experiments and models of fold development in multilayer systems (Ramberg, 1963, 1964; Biot, 1964; see also Williams and Schoneveld, 1981), in which small-scale folds develop in fine layering prior to larger-scale buckling. It has been indirectly verified in the field with the help of strain markers such as sand volcanoes or organic borings parallel to the new cleavage (Nickelsen, 1979; Henderson *et al.*, 1986; Wright and Henderson, 1992).

We are able to present further evidence based on the local overprinting of a low-angle  $S_2$  by tight-gentle, S-asymmetrical  $F_3$  crenulations on the western Threehouse limb (Fig. 4e). During sinistral layer-parallel  $F_2$  and  $F_3$  shearing,  $S_2$  was always in the instantaneous extensional field (Fig. 6d), and thus no crenulations could develop in response to layer-parallel shear. However, as pointed out above, crenulations do occur locally on the western limb. We believe that this crenulation of low-angle  $S_2$  could only have resulted from  $F_3$  layer-parallel shortening prior to major  $F_3$  folding. During subsequent large-scale buckling, when layer-parallel shear became effective in the incompetent layers,  $F_3$  crenulations were tightened and forced to become asymmetrical on the eastern limb and crenulations on the western limb were mostly unfolded (cf. Williams and Schoneveld, 1981, p. 329). The unfolded  $S_2$  continued rotation towards parallelism with lithological layering. We regard this timing of crenulation formation as generally applicable in anisotropic rocks with a penetrative cleavage on the scale of a macroscopic fold, including the initiation of  $S_2$  in the Snow Lake area.

For the following determination of the timing of metamorphism with respect to deformation, only samples and locations from the eastern Threehouse limb are considered, since this is the only place where  $F_2$  and  $F_3$  strains can be distinguished.

### SEQUENCE OF PORPHYROBLAST GROWTH— EVIDENCE FROM INCLUSION TRAILS

In the Burntwood Suite, the presence of  $S_1$  in the



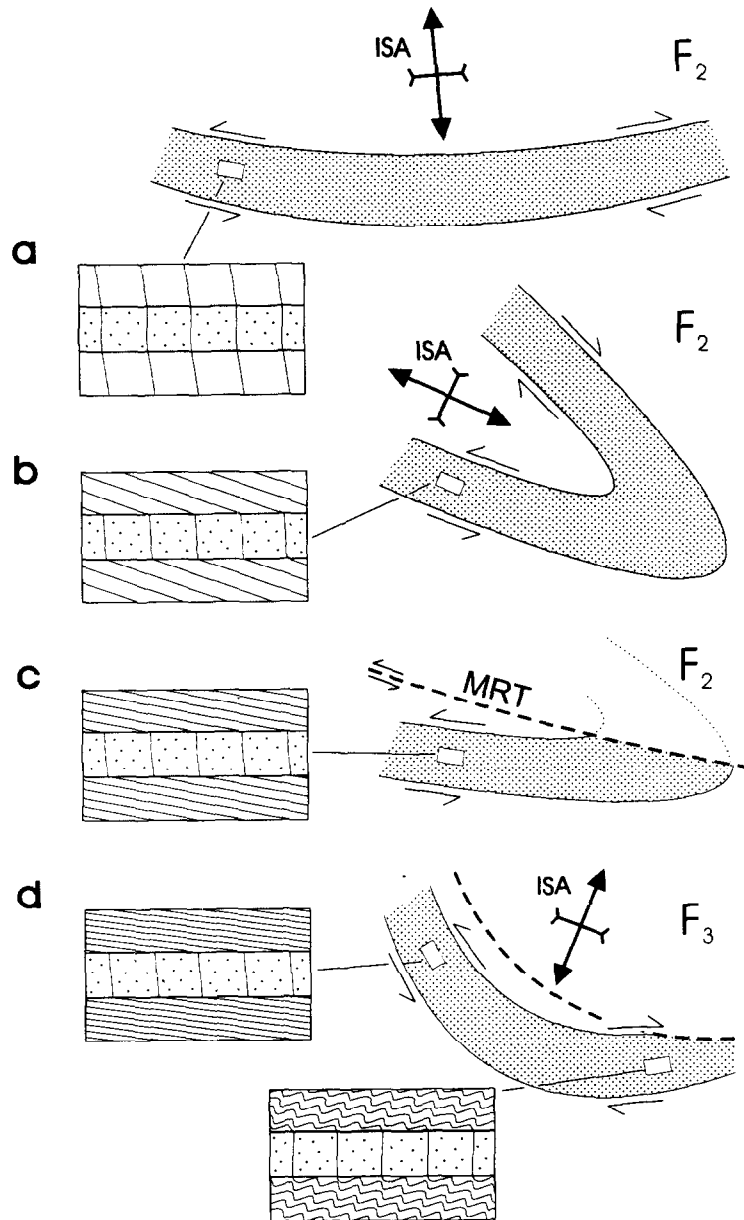
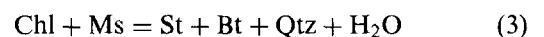
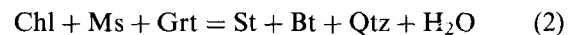


Fig. 6. Sequential development of folding and cleavage during  $F_2$  and  $F_3$ . (a)  $S_2$  initiation during  $F_2$  layer-parallel shortening and early buckling. (b) Subsequent  $S_2$  refraction during fold amplification. (c) The  $F_2$  structure becomes dismembered by the McLeod Road thrust. (d) The relict lower  $F_2$  limb is refolded by the  $F_3$  Threehouse synform. During (d) the low-angle  $S_2$  experiences differential overprinting on both  $F_3$  limbs. ISA = instantaneous stretching axes of the bulk flow.

porphyroblasts makes it possible to establish the sequence of porphyroblast growth and also to examine early increments of  $S_2$  development. Generally, there are two independent lines of evidence for the order of porphyroblast growth, (1) variations in  $S_i$  morphologies in different porphyroblast phases adjacent to each other, and (2) metamorphic textures, such as inclusions of one index mineral in another, dissolution of grain boundaries by metamorphic reactions, and pseudomorphic relationships. Based on metamorphic textures, the following reaction sequence for the Burntwood Suite at Snow Lake during heating was inferred (Froese and Gasparrini, 1975; Kraus and Menard, 1995):



(mineral abbreviations after Kretz, 1983). This order of porphyroblast growth was tested on the  $S_i$  geometries.  $S_i$  is defined by graphite and/or deformed quartz and is generally sub-parallel in adjacent porphyroblast phases (Figs 4b–d, 5, 7b & c). Quartz-inclusions have a shape fabric and are smaller than matrix quartz (Fig. 7b). Locally,  $S_i$  appears parallel to bedding; however it is inclined at high angles to  $S_0$  in the hinges of minor  $F_1$

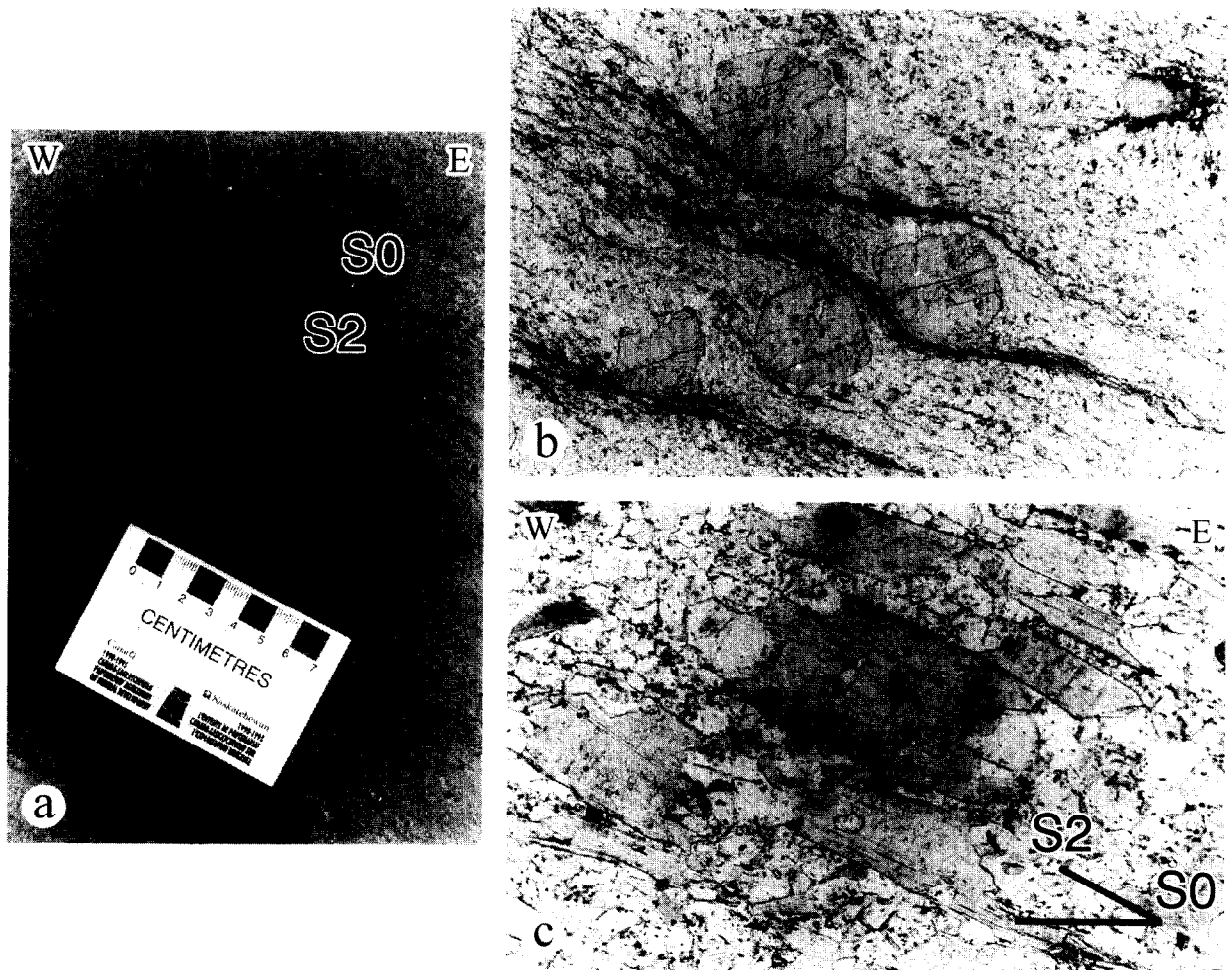


Fig. 7. Bedding-cleavage-porphyroblast relationships on Threehouse east limb. (a) Domainal fabric ( $S_2$ ) in garnetiferous siltstone, only weakly affected by  $F_3$  crenulation. (b) Photomicrograph of (a). Garnet contains planar  $S_1$  ( $= S_1$ ).  $S_2$  septa are partly dissolved. Base is 1 cm. (c) Crystallographically aligned biotites form a low-angle  $S_2$  schistosity. Enveloping muscovite films are not preserved.  $S_0$  is parallel to base of photomicrograph. Base is 1.7 mm. The context of a low  $S_0/S_2$  dihedral angle and planar  $S_1$  at a high angle to  $S_2$  in (b) and (c) indicates rotation of  $S_2$  and porphyroblasts with respect to  $S_0$ . For further explanation see text.

folds (Fig. 5). Therefore,  $S_i$  is a tectonic fabric ( $S_1$ ), which appears to have been axial planar to  $F_1$  structures. Euhedral-subhedral garnet lacks graphite as inclusions and as concentrations around the rims suggesting that graphite was a reactant in reaction (1). In most garnets, the quartz- $S_i$  is planar (Figs 5 & 7b). The generally undeformed biotite grains contain a straight to smoothly curved  $S_i$  mainly of graphite (Figs 4c, d, 5 & 7c). In the quartz-rich, competent beds, where  $S_2$  is sub-orthogonal to  $S_0$ , biotite dimensions and wavelengths of included crenulations are generally larger than in incompetent beds (Fig. 4a). Euhedral to strongly corroded staurolite varies from highly poikiloblastic to inclusion-free depending on the matrix it overgrew. Due to the large staurolite dimensions,  $S_i$ , where present, describes several crenulations within each grain. The  $S_i$  in staurolite is identical in wavelength and composition to the  $S_i$  in the adjacent biotite suggesting simultaneous growth of both phases by reactions (2) and (3).

The different stages of  $F_2$  crenulation development recorded by  $S_i$  in the different porphyroblast phases are

in accord with the above inferred sequence of metamorphic growth and imply that the porphyroblasts grew synkinematically. The constant curvatures of the included crenulations from core to rim further suggest that the porphyroblasts grew rapidly with respect to strain rates. The asymmetry of  $S_i$  in some but not all porphyroblasts indicates that growth occurred when the crenulations in some incompetent beds were constrained to become asymmetrical. Such stages of the  $S_2$  development coincided with  $F_2$  bulk layer-parallel shortening preceding folding and/or during the earlier stages of large-scale fold amplification.

Growth of the porphyroblasts during early  $F_2$  can be confirmed by the timing of their overprinting with respect to folding, the latter giving an upper limit for porphyroblast growth. This is illustrated in Fig. 8(a). In the lower bed, quartz pressure-shadows of some staurolites which are located close to the layer boundary across which cleavage refraction occurs, extend into the adjacent bed, continue tracking the low-angle  $S_2$ , and are crenulated by  $F_3$ . This deflection across lithological boundaries indi-



Fig. 8. Selective overprinting of  $S_2$  on east limb of the Threehouse synform. (a) Lower bed: Staurolite aligned and pulled apart parallel to  $S_2$ . Note the pressure-shadows along  $S_2$  being refracted across the layer boundary. Middle bed: Z-asymmetric  $F_3$  crenulations deforming quartz pressure-shadows of staurolite grains. Upper bed: Strongly poikiloblastic staurolite at base of greywacke bed. For further explanation see text. Younging of beds is to the N. (b) Photomicrograph of  $F_3$  crenulation hinge from (a). High-angle  $S_1/S_2$  relationships are preserved after crenulation.  $S_2$  septa are missing. Note the relict stylolitic residue tracking the former septa. Base is 4.2 mm.

icates that pressure-shadows developed prior to significant  $S_2$  refraction and therefore early during  $F_2$ .

#### INCLUSION TRAIL-CLEAVAGE RELATIONSHIPS—PORPHYROBLAST NON-ROTATION WITH RESPECT TO GEOGRAPHICAL COORDINATES?

Independent of  $S_0/S_2$  dihedral angles,  $S_1$  and  $S_2$  in garnet and biotite are discontinuous and at a high angle to each other everywhere in the Burntwood Suite around Snow Lake (Figs 4b–d, 5, 7b & c). This suggests that garnet and biotite porphyroblasts did not rotate or rotated very little with respect to  $S_2$  during  $F_2$  and  $F_3$ . Such lack of relative rotation between porphyroblast and enveloping cleavage has been interpreted by some workers as indicative of porphyroblast non-rotation with respect to geographical coordinates (e.g. Bell, 1985, 1986; Bell *et al.*, 1992a–c). Nonetheless, in this case, most porphyroblasts rotated in space during folding, because (a) they rotated with respect to  $S_0$  by the same amount as  $S_2$  wherever cleavage refraction occurred in response to  $F_2$  layer-parallel shear, and (b)  $S_0$  itself rotated with respect to geographical coordinates. Thus, different amounts of  $S_2$  refraction resulted in variable  $S_1$  orientations relative to  $S_0$  across layering; however on a small-scale,  $S_1$  in adjacent porphyroblasts remained more or less parallel (Figs 5, 7 & 9). It may be argued that the garnet and biotite overgrew  $S_2$  after folding and therefore did not rotate with respect to any reference frame. This possibility can be ruled out, because the planar geometry of  $S_1$  in many beds, which show small  $S_0/S_2$  dihedral angles, indicates that locally no significant shortening of  $S_1$  had occurred prior to porphyroblast growth (Fig. 7b & c). Whether staurolite rotated relative to  $S_0$  and  $S_e$  cannot be determined with certainty, as most of the specimens do not contain  $S_1$ . In places, where  $S_2$  was subsequently crenulated by  $F_3$ ,  $S_1$  remained sub-orthogonal to the

enveloping  $S_2$ -septa everywhere in the crenulations (Fig. 8b). Non-rotation of porphyroblasts with respect to their enveloping cleavage can therefore not be an argument for non-rotation with respect to geographical coordinates.

#### VEIN-FOLD RELATIONSHIPS

Quartz veins (sub-)parallel to  $S_2$  are ubiquitous throughout the layered sequence. They cut through staurolite porphyroblasts and are locally folded by  $F_3$  crenulations. Depending on the  $S_0/S_2$  angles and thus on lithology, these veins are stubby in the quartzose beds and are rather spindly and locally boudinaged in the mudstones (Fig. 10). In the light of the above observations, we attribute these veins to layer-parallel extension in the advanced stages of  $F_2$  folding (Fig. 10c). Layer-parallel extension was controlled by the  $S_2$  anisotropy and thus was accommodated differently in different lithologies. Rigid competent layers were simply torn apart along high-angle  $S_2$ , whereas pelitic layers were extended by slip along  $S_2$  septa. The large thickness of the stubby veins is a consequence of the relatively low ductility of the competent beds.

#### DEVELOPMENT OF SCHISTOSITY FROM DIFFERENTIATED LAYERING—AN ALTERNATIVE MODEL

As mentioned above, the  $S_2$  morphologies in the metaturbidites record gradations from differentiated layering to a coarse schistosity defined by aligned biotite. This aspect requires further discussion. Schistosity in metamorphosed micaceous pelitic rocks has been reported to develop in several ways. For example, a schistosity which is defined by coarse-grained micas is assumed to have developed during growth of these minerals (Voll, 1960; Tobisch *et al.*, 1970; Dallmeyer

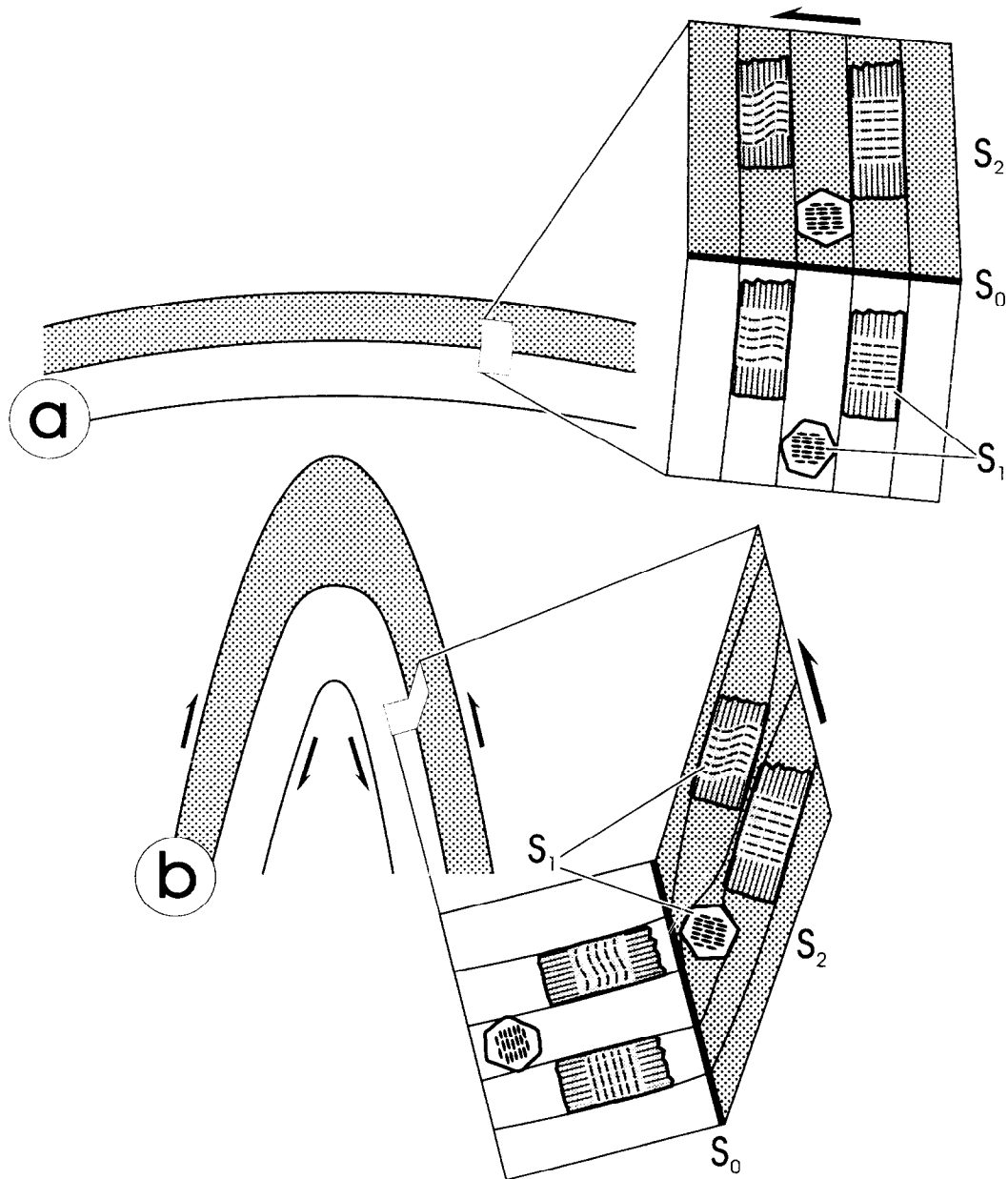


Fig. 9. Schematic summary of bedding-cleavage-porphyroblast relationships during  $F_2$  folding. (a) Garnet and biotite porphyroblasts overgrew an  $S_0$ -parallel  $S_1$  during early  $F_2$  and thus contain straight to smoothly curved  $S_1$ . (b) During fold amplification and  $S_2$  rotation (stippled), the porphyroblasts did not rotate with respect to  $S_2$  in incompetent beds. In competent greywacke (white),  $S_2$  and porphyroblasts did not rotate with respect to  $S_0$ .

*et al.*, 1983). If the bulk of the mica growth predates the cleavage forming event, as in the Burntwood Suite, other mechanisms must account for schistosity formation. Mathematical theories of rigid body rotation of randomly distributed single grains have been proposed by Jeffery (1922) and March (1932). However, their models cannot explain the locally domainal fabric. Alternatively, schistosity may grow from a coarsening crenulation cleavage (e.g. Williams, 1977, 1985) or involve kinking of an earlier foliation (Williams, 1977; Williams *et al.*, 1977; Williams and Compagnoni, 1983) but the continuous  $S_1$  in biotite (see above) also rules out these possibilities (Figs 4b-d & 7c).

Microfabrics, metamorphic textures and phase petrology suggest that the schistosity in the Burntwood Suite developed from the destruction of the domainal cleavage by muscovite removal, preferentially from cleavage septa. Loss of muscovite is indicated by the different preservation states of adjacent cleavage septa in the same micro-bed on the scale of a thin section. Locally, septa (adjacent to well-preserved septa) may have been completely destroyed so that porphyroblasts 'float' freely in a quartz matrix that shows no anisotropy (Fig. 5; see also Figs 7c & 8b). In such domains now devoid of muscovite, the graphite- $S_1$  in biotite porphyroblasts is identical in shape and geometry to biotite  $S_1$  in adjacent domains

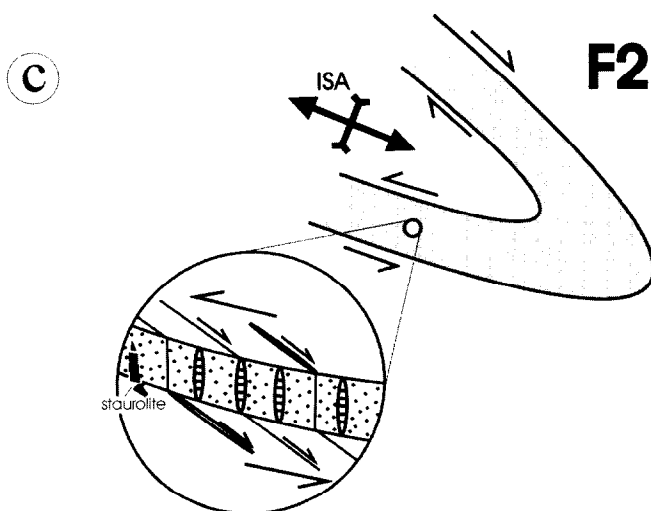
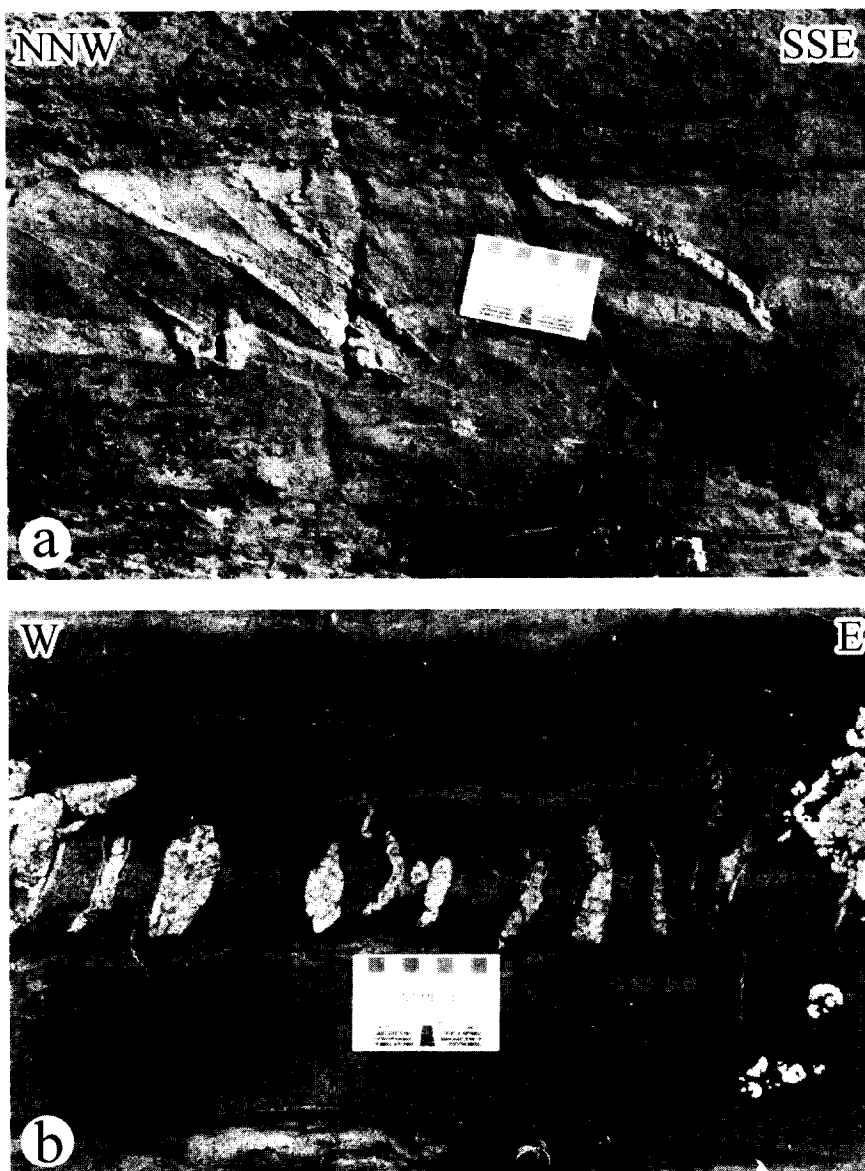


Fig. 10. Late- $F_2$  quartz veins parallel to  $S_2$ . (a) Spindly, boudinaged veins on Threehouse west limb record continual sinistral  $F_2$  and  $F_3$  layer-parallel shear. Anticlockwise rotation of veins is indicated by S-folds in the competent calcisilicate layer at their base. Note stubby vein within the competent layer at the left hand side. (b) Stubby veins with  $S_0$  tightened around them, Threehouse east limb. (c) Sketch showing vein developed during  $F_2$  folding.

where the septa are preserved (Fig. 5) suggesting that a layered anisotropy existed in both types of domain during porphyroblast growth. Here, the schistosity is defined by trains of well-aligned biotite, which are the loci of the former microlithons, in a coarsened quartz matrix (Figs 4a, 5 & 7c). The local demise of  $S_2$  septa indicates that schistosity developed after  $S_2$  differentiation and after growth of the prograde metamorphic assemblage. Muscovite dissolution endured until syn- or post- $F_3$  as recorded by skeletal  $F_3$  crenulations, in which only the aligned biotite porphyroblasts are preserved (Fig. 8b). We believe that muscovite was dissolved by fluids and was flushed out of the system. During fluid infiltration,  $S_2$  septa acted possibly as channels of enhanced fluid flow in a way described by Williams (1990). Evidence of fluid activity is given by the deficiency of matrix muscovite in many samples and by the local corrosion of biotite and staurolite rims in the absence of a higher grade aluminosilicate forming reaction. Chlorite and muscovite participated in reactions (2) and (3), and muscovite must have been left over when the reactions stopped. The presence of these phyllosilicates prior to reactions (2) and (3) is also indicated by their inclusion in porphyroblasts. Although Al, as contained in the muscovite, is considered to be relatively immobile (Carmichael, 1969), it is suggested that Al was flushed out of the system by high-pH fluids (Kraus and Menard, 1995; see also Glen, 1979 and Mancktelow, 1994). This interpretation correlates with a widespread fluid activity in the adjacent Snow Lake assemblage during  $F_2$  and  $F_3$  causing syntectonic alteration of volcanic-hosted massive sulphide deposits (Menard and Gordon, 1995, 1997).

## SYNTHESIS AND CONCLUSIONS

In the Burntwood Suite metaturbidites at Snow Lake, a single penetrative cleavage,  $S_2$ , is ubiquitously developed as a domainal fabric, which shows all gradations into a schistosity. The fabric developed from crenulation of a bedding-parallel  $S_1$ , which formed during  $F_1$  isoclinal folding at 1.84 Ga. Such crenulations are included as  $S_1$  in porphyroblasts of staurolite and biotite. These porphyroblasts grew between 1.815 Ga and 1.8 Ga, when  $F_2$  crenulations were constrained in some incompetent layers to become asymmetrical prior to  $F_2$  fold tightening during a very small deformation increment. Associated peak conditions of metamorphism were 560–570°C and ~4–4.5 kbar. Local transformation of the differentiated layering into a schistosity by muscovite dissolution endured until syn- or post- $F_3$  after 1.8 Ga. In incompetent beds,  $S_2$  and porphyroblasts rotated with respect to  $S_0$  during  $F_2$  tightening on the presently exposed limb of the  $F_2$  McLeod Lake fold. However, they did not rotate relative to one another (in micro-beds on the scale of a thin section) and remained more or less stationary with respect to  $S_0$  in competent beds. Layer-parallel extension during the later stages of  $F_2$  was accommodated by

separation along  $S_2$  in the competent beds, resulting in quartz vein formation.  $S_2$  and porphyroblast pressure-shadows, where favourably oriented, were crenulated prior to  $F_3$  large-scale folding.  $F_3$  crenulations were accentuated by dextral layer-parallel shear on the eastern limb of the Threehouse synform and unfolded by continued sinistral layer-parallel shear on the western limb. As a result, the initial developmental stages of an  $S_3$  is preserved on the eastern  $F_3$  limb only. On the other limb,  $S_2$  was largely unaltered, and after rotation associated with  $F_3$  appears axial planar to the  $F_3$  structure.

Our work supports the hypothesis that in areas of polydeformed anisotropic micaceous pelitic rocks, cleavage may start to develop prior to folding. In general, domainal cleavage develops whenever microfolding is possible. Whether and when microfolding takes place during large-scale folding strongly depends on the orientation of the anisotropy to be crenulated with respect to layering. In special circumstances, a cleavage may develop late. For example, in a setting such as the west limb of the Threehouse synform, where a pervasive new cleavage does not form because of the orientation of the old cleavage, a local cleavage may form late during folding in the hinges of minor folds. The Threehouse synform example also shows that a domainal cleavage may develop locally, for example on one fold limb only, and there only in selected layers depending on the orientation of the previous fabric. As crenulation and differentiation involve the destruction of the previous fabric (e.g. Tobisch and Paterson, 1988; this work) the only foliation present in alternating lithologies may be of different generations. This has implications for other areas, for example the Slave Province, Canada, where, in the Yellowknife Supergroup metaturbidite sequence, two subsequent, however morphologically similar fabrics alternate in adjacent beds, displaying a chevron pattern (Fyson, 1982, 1984; Henderson, 1997). This pattern possibly formed by the same mechanisms operating in the Threehouse synform area with the difference that, in the Yellow Knife supergroup, the later fabric experienced complete differentiation.

*Acknowledgements*—We are grateful to Al Bailes and Al Galley for their introduction to and discussion of the geology of the Snow Lake area. Jim Ryan, Dazhi Jiang, Thomas Menard and Steve Lucas are also thanked for stimulating discussions. Excellent thin sections were prepared by Dave Pirie, Ancel Murphy and Calvin Nash. Angel Gomez digitally assembled the photoplates. Steve Lucas, the Geological Survey of Canada, the Manitoba Energy and Mines Department and numerous helpful people in Snow Lake are thanked for logistical support. This project was largely funded by an NSERC operating grant awarded to P.F.W. We would like to dedicate this paper to the late Jack Henderson.

## REFERENCES

- Ansdell, K. M. (1993) U–Pb zircon constraints on the timing and provenance of fluvial sedimentary rocks in the Flin Flon and Athapapuskow basins, Flin Flon Domain, Trans-Hudson Orogen,

- Manitoba and Saskatchewan. In *Radiogenic Age and Isotopic Studies: Report 7, Geological Survey of Canada Paper 93-2*, pp. 49–57.
- Bailes, A. H. (1980) Origin of Early Proterozoic volcanoclastic turbidites, south margin of the Kiseynew sedimentary gneiss belt, File Lake, Manitoba. *Precambrian Research* **12**, 197–225.
- Bailes, A. H. and McRitchie, W. D. (1978) The transition from low to high grade metamorphism in the Kiseynew sedimentary gneiss belt, Manitoba. In *Metamorphism in the Canadian Shield. Geological Survey of Canada Paper 78-10*, pp. 155–178.
- Bell, T. H. (1985) Deformation partitioning and porphyroblast rotation in metamorphic rocks: a radical reinterpretation. *Journal of Metamorphic Geology* **3**, 109–118.
- Bell, T. H. (1986) Foliation development and refraction in metamorphic rocks: reactivation of earlier foliations and decrenulation due to shifting patterns off deformation partitioning. *Journal of Metamorphic Geology* **4**, 421–444.
- Bell, T. H., Forde, A. and Hayward, N. (1992a) Do smoothly curved, spiral-shaped inclusion trails signify porphyroblast rotation? *Geology* **20**, 59–62.
- Bell, T. H., Johnson, S. E., Davis, B., Forde, A., Hayward, N. and Wilkins, C. (1992b) Porphyroblast inclusion-trail orientation data: eppure non son girate! *Journal of Metamorphic Geology* **10**, 295–307.
- Bell, T. H., Forde, A. and Hayward, N. (1992c) Reply on “Do smoothly curved, spiral-shaped inclusion trails signify porphyroblast rotation?”. *Geology* **20**, 1055–1056.
- Bell, T. H., Rubenach, M. J. and Fleming, P. D. (1986) Porphyroblast nucleation, growth and dissolution in regional metamorphic rocks as a function of deformation partitioning during foliation development. *Journal of Metamorphic Geology* **4**, 37–67.
- Berman, R. G. (1988) Internally-consistent thermodynamic data for minerals in the system  $\text{Na}_2\text{O}-\text{K}_2\text{O}-\text{CaO}-\text{MgO}-\text{FeO}-\text{Fe}_2\text{O}_3-\text{Al}_2\text{O}_3-\text{SiO}_2-\text{TiO}_2-\text{H}_2\text{O}-\text{CO}_2$ . *Journal of Petrology* **29**, 445–552.
- Berman, R. G. (1990) Mixing properties of Ca-Mg-Fe-Mn garnets. *American Mineralogist* **75**, 328–344.
- Berman, R. G. (1991) Thermobarometry using multi-equilibrium calculations: a new technique, with petrological applications. *Canadian Mineralogist* **29**, 833–855.
- Berman, R. G. and Koziol, A. M. (1991) Ternary excess properties of grossular-pyrope-almandine garnets and their influence in geothermobarometry. *American Mineralogist* **76**, 1223–1231.
- Biot, M. A. (1964) Theory of internal buckling of a confined multi-layered structure. *Geological Society of America Bulletin* **75**, 563–568.
- Bleeker, W. (1990) New structural-metamorphic constraints on Early Proterozoic oblique collision along the Thompson Nickel Belt, Manitoba, Canada. In *The Early Proterozoic Trans-Hudson Orogen of North America*, ed. J. F. Lewry and M. R. Stauffer, Vol. 37, pp. 57–73. *Geological Association of Canada Special Paper*.
- Carmichael, D. M. (1969) On the mechanism of prograde metamorphic reactions in quartz-bearing pelitic rocks. *Contributions to Mineralogy and Petrology* **20**, 244–267.
- Connors, K. A. (1996) Unraveling the boundary between turbidites of the Kiseynew belt and volcano-plutonic rocks of the Flin Flon belt Trans-Hudson Orogen, Canada. *Canadian Journal of Earth Sciences* **33**, 811–829.
- Dallmeyer, R. D., Kean, B. F., Odom, A. L. and Jayasinghe, N. R. (1983) Age and contact-metamorphic effects of the Overflow Pond Granite: an undeformed pluton in the Dunnage Zone of the Newfoundland Appalachians. *Canadian Journal of Earth Sciences* **20**, 1639–1645.
- David, J., Bailes, A. H. and Machado, N. (1996) Evolution of the Snow Lake portion of the Paleoproterozoic Flin Flon and Kiseynew belts, Trans-Hudson Orogen, Manitoba, Canada. *Precambrian Research* **80**, 107–124.
- Froese, E. and Gasparri, E. (1975) Metamorphic zones in the Snow Lake area, Manitoba. *Canadian Mineralogist* **13**, 162–167.
- Froese, E. and Moore, J. M. (1980) Metamorphism in the Snow Lake area, Manitoba. *Geological Survey of Canada Paper*, 78–27.
- Fuhrman, M. L. and Lindsley, D. H. (1988) Ternary-feldspar modeling and thermometry. *American Mineralogist* **73**, 201–215.
- Fyson, W. K. (1982) Complex evolution of folds and cleavages in Archean rocks, Yellowknife, N.W.T. *Canadian Journal of Earth Sciences* **19**, 878–893.
- Fyson, W. K. (1984) Basement-controlled structural fronts forming an apparent major refold pattern in the Yellowknife domain, Slave Province. *Canadian Journal of Earth Sciences* **21**, 822–828.
- Galley, A. G., Ames D. E. and Franklin, J. M. (1988) Geological setting of gold mineralization, Snow Lake, Manitoba. *Geological Survey of Canada Open File 1700*.
- Glen, R. A. (1979) Evidence for cyclic reactions between andalusite, ‘sericite’ and sillimanite, Mount Franks area, Willyama Complex, N.S.W. *Tectonophysics* **58**, 97–112.
- Gordon, T. M., Hunt, P. A., Bailes, A. H. and Syme, E. C. (1990) U–Pb ages of the Flin Flon and Kiseynew Domains, Manitoba: chronology of crust formation at an Early Proterozoic accretionary margin. In *The Early Proterozoic Trans-Hudson Orogen of North America*, ed. J. F. Lewry and M. R. Stauffer, Vol. 37, pp. 177–199. *Geological Association of Canada Special Paper*.
- Henderson, J. R. (1997) Development of a chevron cleavage pattern and porphyroblast rotation in graded metaturbidites, Slave structural province, Northwest Territories, Canada. *Journal of Structural Geology* **19**, 653–661.
- Henderson, J. R., Wright, T. O. and Henderson, M. N. (1986) A history of cleavage and folding: an example from the Goldenville Formation, Nova Scotia. *Geological Society of America Bulletin* **97**, 1354–1366.
- Hobbs, B. E., Means, W. D. and Williams, P. F. (1976) *An Outline of Structural Geology*. Wiley, New York.
- Hodges, K. V. and Crowley, P. D. (1985) Error estimation and empirical geothermobarometry for pelitic systems. *American Mineralogist* **70**, 702–709.
- Hoepfner, R. (1956) Zum Problem der Bruchbildung, Schieferung und Faltung. *Geologische Rundschau* **45**, 247–283.
- Hoffman, P. F. (1988) United plates of America, the birth of a craton: Early Proterozoic assembly and growth of Laurentia. *Annual Reviews of Earth and Planetary Sciences* **16**, 543–603.
- Hoisch, T. D. (1990) Empirical calibration of six geobarometers for the mineral assemblage quartz + muscovite + biotite + plagioclase + garnet. *Contributions to Mineralogy and Petrology* **104**, 225–234.
- Jeffery, G. B. (1922) The motion of ellipsoidal particles immersed in a viscous fluid. *Royal Society of London Proceedings Series A* **102**, 161–177.
- Johnson, S. E. and Vernon, R. H. (1995) Inferring the timing of porphyroblast growth in the absence of continuity between inclusion trails and matrix foliations: can it be reliably done? *Journal of Structural Geology* **17**, 1203–1206.
- Kienow, S. (1942) Grundzüge einer Theorie der Faltungs- und Schieferungsvorgänge. *Fortschritte der Geologie und Paläontologie* **14**, 1–129.
- Kleemann, U. and Reinhardt, J. (1994) Garnet-biotite thermometry revisited: The effect of  $\text{Al}^{\text{VI}}$  and Ti in biotite. *European Journal of Mineralogy* **6**, 925–941.
- Knipe, R. J. (1981) The interaction of deformation and metamorphism in slate. *Tectonophysics* **78**, 249–272.
- Knipe, R. J. and White, S. H. (1977) Microstructural variation of an axial plane cleavage around a fold—a high voltage electron microscope study. *Tectonophysics* **39**, 355–380.
- Kraus, J. and Menard, T. (1995) Metamorphism of the File Lake Formation, Snow Lake: Preliminary results. Manitoba Energy and Mines, Minerals Division, Report of Activities, pp. 160–163.
- Kraus, J. and Menard, T. (1997) A thermal gradient at constant pressure: implications for low- to medium-pressure metamorphism in a compressional tectonic setting, Flin Flon and Kiseynew Domains, Trans-Hudson Orogen, Central Canada. In *Tectono-metamorphic Studies in the Canadian Shield—part I*, ed. R. G. Berman and R. M. Easton. *Canadian Mineralogist* **35**, 1117–1136.
- Kraus, J. and Williams, P. F. (1994a) Structure of the Squall Lake area, Snow Lake (NTS 63K/16). *Manitoba Energy and Mines, Minerals Division, Report of Activities*, 1994, pp. 189–193.
- Kraus, J. and Williams, P. F. (1994) Cleavage development and the timing of metamorphism in the File Lake Formation across the Threehouse synform, Snow Lake, Manitoba: A new paradigm. *Lithoprobe Trans-Hudson Orogen Transect Report* **38**, 230–237.
- Kraus, J. and Williams, P. F. (1995) The tectonometamorphic history of the Snow Lake area, Manitoba, revisited. *Lithoprobe Trans-Hudson Orogen Transect Report* **48**, 206–212.
- Kretz, R. (1983) Symbols for rock-forming minerals. *American Mineralogist* **68**, 277–279.
- Lewry, J. F. and Stauffer, M. R. (editors) (1990) The Early Proterozoic Trans-Hudson Orogen of North America. *Geological Association of Canada Special Paper* 37.
- Lister, G. S. and Williams, P. F. (1983) The partitioning of deformation in flowing rock masses. *Tectonophysics* **92**, 1–33.
- Lucas, S. B., Stern, R. A., Syme, E. C., Reilly, B. A. and Thomas, D. J. (1996) Intraoceanic tectonics and the development of continental

- crust: 1.92–1.84 Ga evolution of the Flin Flon Belt, Canada. *Geological Society of America Bulletin* **108**, 602–629.
- Mäder, U. K., Percival, J. A. and Berman, R. G. (1994) Thermobarometry of garnet–clinopyroxene–hornblende granulites from the Kapuskasing structural zone. *Canadian Journal of Earth Sciences* **31**, 1134–1145.
- Mancktelow, N. S. (1994) On volume change and mass transport during the development of crenulation cleavage. *Journal of Structural Geology* **16**, 1217–1231.
- March, A. (1932) Mathematische Theorie der Regelung nach der Korngestalt bei affiner Deformation. *Zeitschrift für Kristallographie, Kristallgeometrie und Kristallphysik* **81**, 285–297.
- Marlow, P. C. and Etheridge, M. A. (1977) Development of a layered crenulation cleavage in mica-schists of the Kanmantoo Group near Macclesfield, South Australia. *Geological Society of America Bulletin* **88**, 873–882.
- McMullin, D. W. A., Berman, R. G. and Greenwood, H. J. (1991) Calibration of the SGAM thermobarometer for pelitic rocks using data from phase equilibrium experiments and natural assemblages. *Canadian Mineralogist* **29**, 889–908.
- Menard, T. and Gordon, T. M. (1995) Syntectonic alteration of VMS deposits, Snow Lake, Manitoba. *Manitoba Energy and Mines, Minerals Division, Report of Activities*, 1995, pp. 164–167.
- Menard, T. and Gordon, T. M. (1997) Metamorphic P–T paths from the eastern Flin Flon Belt and Kiseynew Domain, Snow Lake, Manitoba. In *Tectono-metamorphic Studies in the Canadian Shield—part I*, ed. R. G. Berman and R. M. Easton. *Canadian Mineralogist* **35**, 1093–1115.
- Nickelsen, R. P. (1979) Sequence of structural stages of the Alleghany Orogeny, at the Bear Valley Strip Mine, Shamokin, Pennsylvania. *American Journal of Science* **279**, 225–271.
- Parent, M., Machado, N. and Zwanzig, H. (1995) Timing of metamorphism and deformation in the Jungle Lake area, southern Kiseynew belt, Manitoba: evidence from U–Pb geochronology of monazite and zircon. *Lithoprobe Trans-Hudson Orogen Transect Report* **48**, 131–132.
- Passchier, C. W., Trouw, R. A. J., Zwart, H. J. and Vissers, R. L. M. (1992) Porphyroblast rotation: eppur si muove? *Journal of Metamorphic Geology* **10**, 283–294.
- Powell, R. and Holland, T. J. B. (1988) An internally consistent dataset with uncertainties and correlations: 3. Applications to geobarometry, worked examples and a computer program. *Journal of Metamorphic Geology* **6**, 173–204.
- Ramberg, H. (1963) Evolution of drag folds. *Geological Magazine* **100**, 97–106.
- Ramberg, H. (1964) Selective buckling of composite layers with contrasted rheological properties, a theory for simultaneous formation of several orders of folds. *Tectonophysics* **1**, 307–341.
- Rickard, M. J. (1961) A note on cleavages in crenulated rocks. *Geological Magazine* **98**, 324–332.
- Russell, G. A. (1957) Structural studies of the Snow Lake–Herb Lake area. Herb Lake Mining Division, Manitoba. *Manitoba Mines Branch Publication* 55–3.
- Stauffer, M. R. (1990) The Missi Formation: an Apehian molasse deposit in the Reindeer Lake Zone of the Trans-Hudson Orogen, Canada. In *The Early Proterozoic Trans-Hudson Orogen of North America*, ed. J. F. Lewry and M. R. Stauffer, Vol. 37, pp. 121–141. *Geological Association of Canada Special Paper*.
- Stern, R. A., Syme, E. C., Baines, A. H. and Lucas, S. B. (1995) Paleoproterozoic (1.90–1.86 Ga) arc volcanism in the Flin Flon Belt, Trans-Hudson Orogen, Canada. *Contributions to Mineralogy and Petrology* **119**, 117–141.
- Spry, A. (1969) *Metamorphic Textures*. Pergamon Press, Oxford.
- Tobisch, O. T., Fleuty, M. J., Merth, S. S., Mukhopadhyay, D. and Ramsay, J. G. (1970) Deformational and metamorphic history of the Moianian and Lewisian rock between Strathconon and Glenaffric. *Scottish Journal of Geology* **6**, 243–265.
- Tobisch, O. T. and Paterson, S. R. (1988) Analysis and interpretation of composite foliations in areas of progressive deformation. *Journal of Structural Geology* **10**, 745–754.
- Vernon, R. H. (1977) Relationships between microstructures and metamorphic assemblages. *Tectonophysics* **39**, 439–452.
- Vernon, R. H. (1978) Porphyroblast-matrix microstructural relationships in deformed metamorphic rocks. *Geologische Rundschau* **67**, 288–305.
- Vernon, R. H. (1988) Microstructural evidence of rotation and non-rotation of mica porphyroblasts. *Journal of Metamorphic Geology* **6**, 595–601.
- Vernon, R. H. (1989) Porphyroblast–matrix microstructural relationships: recent approaches and problems. In *Evolution of metamorphic belts*, ed. J. S. Daly, R. A. Cliff and B. W. D. Yardley, pp. 83–102. *Special Publications of the Geological Society of London* 43.
- Voll, G. (1960) New work on petrofabrics. *Liverpool Manchester Geological Journal* **2**, 503–567.
- Weber, K. (1976) Gefügeuntersuchungen an transversalgeschieften Gesteinen aus dem östlichen Rheinischen Schiefergebirge (Ein Beitrag zur Genese der transversalen Schieferung). *Geologisches Jahrbuch Reihe D* **15**, 1–99.
- Weber, K. (1981) Kinematic and metamorphic aspects of cleavage formation in very low-grade metamorphic slates. *Tectonophysics* **78**, 291–306.
- Williams, P. F. (1972) Development of metamorphic layering and cleavage in low-grade metamorphic rocks at Bermagui, Australia. *American Journal of Science* **272**, 1–47.
- Williams, P. F. (1977) Foliation: a review and discussion. *Tectonophysics* **39**, 305–328.
- Williams, P. F. (1979) The development of asymmetrical folds in a cross-laminated siltstone. *Journal of Structural Geology* **1**, 19–30.
- Williams, P. F. (1985) Multiply deformed terrains—problems of correlation. *Journal of Structural Geology* **7**, 269–280.
- Williams, P. F. (1990) Differentiated layering in metamorphic rocks. *Earth Science Reviews* **29**, 267–281.
- Williams, P. F. and Compagnoni, R. (1983) Deformation and metamorphism in the Bard area of the Sesia Lanzo Zone, Western Alps, during subduction and uplift. *Journal of Metamorphic Geology* **1**, 117–140.
- Williams, P. F., Means, W. D. and Hobbs, B. E. (1977) Development of axial-plane slaty cleavage and schistosity in experimental and natural materials. *Tectonophysics* **42**, 139–158.
- Williams, P. F. and Schoneveld, C. (1981) Garnet rotation and the development of axial plane crenulation cleavage. *Tectonophysics* **78**, 307–334.
- Wright, T. O. and Henderson, J. R. (1992) Volume loss during cleavage formation in the Meguma Group, Nova Scotia, Canada. *Journal of Structural Geology* **14**, 281–290.
- Zwanzig, H. V. (1990) Kiseynew Gneiss Belt in Manitoba: stratigraphy, structure and tectonic evolution. In *The Early Proterozoic Trans-Hudson Orogen of North America*, ed. J. F. Lewry and M. R. Stauffer, pp. 95–120. *Geological Association of Canada Special Paper* 37.
- Zwart, H. J. (1960) The chronological succession of folding and metamorphism in the Central Pyrenees. *Geologische Rundschau* **50**, 203–218.
- Zwart, H. J. (1962) On the determination of polymetamorphic mineral associations, and its application to the Bosost area (Central Pyrenees). *Geologische Rundschau* **52**, 38–65.